

# System noise of a digital pulse processing module for nuclear instrumentation

Y. Ma, W.-J. Fischer, J. Henniger, D. Weinberger, T. Kormoll  
TU Dresden, Germany  
yuzhen.ma@tu-dresden.de

**Abstract**—Digital pulse processing finds a widespread use in nuclear instrumentation. This work presents a digital pulse processing (DPP) module based on an FPGA and a 16-bit 125 MHz ADC and analyses the system noise distribution by acquired digital data using this system. A moving average filter is utilized to suppress the system noise of the DPP module. Furthermore, digital trapezoidal filter is applied for the use with a charge sensitive preamplifier with High Purity Germanium (HPGe) detector. The energy spectrum and corresponding resolution are demonstrated with a scintillation and semiconductor detector.

**Index Terms**—digital signal processing; FPGA; noise; Gaussian; nuclear

## I. INTRODUCTION

Digital pulse processing (DPP) has been widely used in the ionizing radiation field recently. It has many advantages compared to analog system in the development phase and update period [1]. DPP modules have become more and more popular during the past decades since the development of semiconductor and digital components, such as Field Programmable Gate Arrays (FPGAs) and high-speed analog-to-digital converters (ADCs). The amplifier and ADC are assigned to accurately and reliably amplify or sample the amplitude of a continuous voltage pulse that can be subject to various noise sources [2]. Amplitude depends not only on the system noise, but also on the instantaneous value of the offset, which is very critical for a nuclear instrumentation for it is proportional to the amount of charge.

In the present paper, a DPP module is handled, which contains a free-running sampling ADC and an FPGA for real-time pulse analysis. In this work, the system response to signals from a pulse generator and radiation detectors are investigated.

## II. MATERIAL AND METHODS

A digital spectroscopy system contains detector, processor and analyzer, which aims to receive, process and analyze ionizing radiation on event-by-event traces [3], [4]. Most

Y. Ma and W. Fischer are with the MST (Institute of Semiconductor and Microsystems Technology), Technische Universität Dresden, Dresden 01069, Germany (e-mail: Yuzhen.Ma@tu-dresden.de, Wolf-Joachim.Fischer@tu-dresden.de).

J. Henniger is with the IKTP (Institute of Nuclear and Particle Physics), Technische Universität Dresden, Dresden 01069, Germany (e-mail: henniger@asp.tu-dresden.de).

D. Weinberger is with the HZDR (Helmholtz-Zentrum Dresden-Rossendorf), Dresden 01328, Germany and Serious Dynamics GbR, Dresden 01139, Germany (e-mail: weinberger@serious-dynamics.de)

T. Kormoll is with the IKTP (Institute of Nuclear and Particle Physics), Technische Universität Dresden, Dresden 01069, Germany and Serious Dynamics GbR, Dresden 01139, Germany (Thomas.Kormoll@tu-dresden.de)

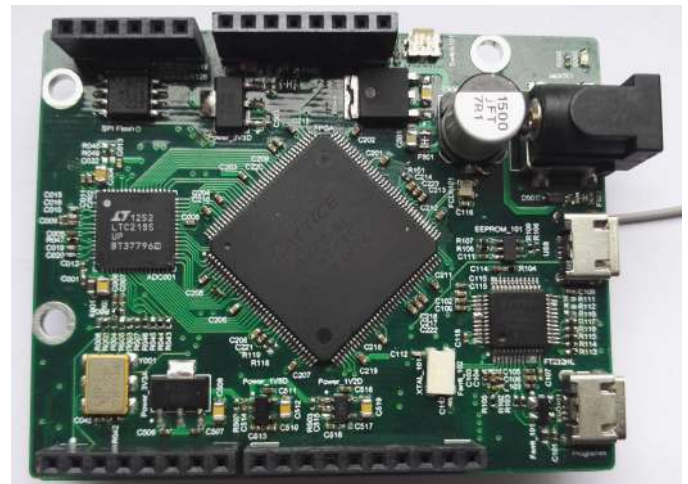


Fig. 1. Hardware design based on a LatticeXP2 FPGA.

common features of an event scintillation detector are energy, time and pulse shape.

### A. Design of the digital signal processing system

The DPP architecture described hereafter is called DAQ125 that is a 2-channel, 125 MHz 16-bit digitizer board as shown in figure 1. It has three stages, analogue input, digital processing, and uploading data for analysis. The whole system block is depicted in figure 2, in which these three stages are represented by three different kinds of background colors respectively. In the first stage, an RC lowpass filter acting as an anti-aliasing filter isolates the drive circuitry from the A/D sample-and/hold switching, and limits wideband noise from the drive circuitry. 25  $\Omega$  resistor and 12 pF capacitor are chosen as the values of lowpass filter components based on the input radiation signal frequency [5]. The continuous signal from a radiation detector is sampled by the ADC LTC2185 and processed by the FPGA LatticeXP2 in real-time. In the second stage, the acquired data stream is passed to an FPGA firmware which comprises digital modules, i.e., trigger, shift register, waveform memory, integrator and control-memory. The FPGA firmware is self-triggering and allows to readout a portion of waveform around the trigger point or to calculate some features around the trigger and to transfer only certain numbers per event. The trigger mode of this firmware is leading or falling edge and the threshold value is within the input range of ADC. The delaying length of the trigger point is controlled by a shift register that is configured through software. Once input

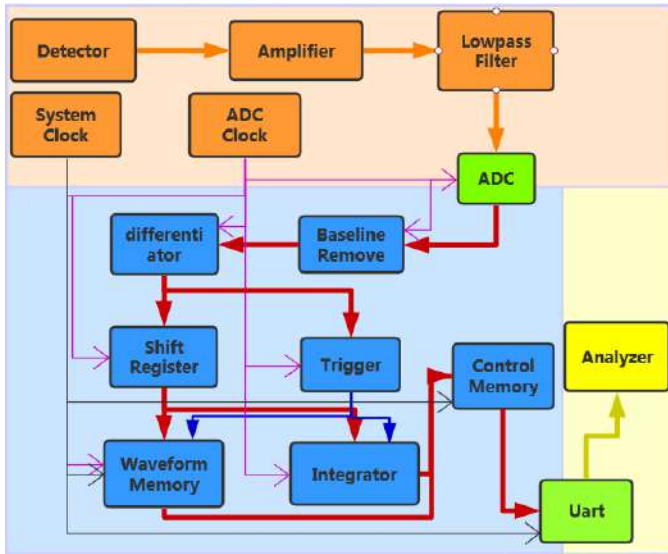


Fig. 2. Architectural block of whole system.

data is triggered and shifted, the transferred data is saved into waveform memory up to a maximum amount of 512 samples.

### B. Reference system

The acquired data from an oscilloscope HDO4000A of Teledyne LeCroy is used as a reference comparing to the output of the designed DAQ125 to evaluate and analyze execution of the designed DPP system. Both of these two schemes are connected to a pulse generator or detector by using a BNC-KJK connector simultaneously. The sampling rate of HDO4000A is 10GSPS with 5  $\mu$ s sampling time per analyzing data stream. Corresponding to the sampling rate and sampling time of LTC2185 ADC, 512 samples are extracted from the raw data of HDO4000A by extracting one sample every 80 times to work as a reference for the acquired data by using DAQ125. In order to get the distribution curve of noise, Probability Distribution Function (PDF) is employed to analyze the characteristic of system noise.

In the primary phase, a pulse generator, TR-0458/B, is utilized. The parameters of the generated signal such as waveform, frequency, amplitude and duty cycle can be manual changed. In this work, a pulse signal with a frequency of 1 MHz, a amplitude of -4 dBV and a duty cycle of 37.2% is generated.

At the last stage, the scintillation detector CeBr<sub>3</sub> and semiconductor detector HPGe are employed. A dual digital multichannel analyzer (MCA) of CAEN S.p.A. is utilized as a reference which is comparing to the spectroscopy of the DPP to evaluate its performance. The HPGe detector is biased by the 2000 V high voltage with 300  $\mu$ A current using one channel of module MCA DT5780. The software MC<sup>2</sup> Analyzer is utilized to acquire data and plot energy spectrum in real time with the energy filter setup that 8  $\mu$ s rise time, 48.34  $\mu$ s decay time, 2.5  $\mu$ s flat top and 80% flat top delay. The sampling rate of DT5780 is 100MS/s with 14-bit for analyzing data. 512 samples are extracted from the raw data of DAQ125

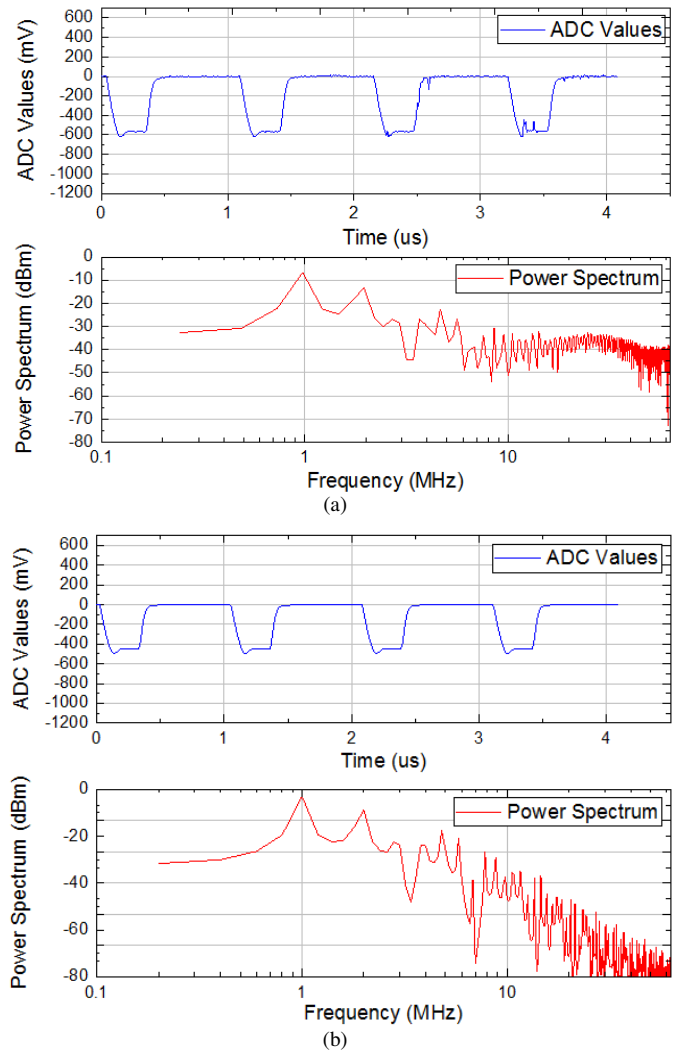


Fig. 3. Acquired data (a) and reference signal (b) shown in time and frequency domain acquired by HDO4000A. The total measurement is 512 samples.

according to the sampling rate of LTC2185 ADC and output signal of HPGe detector.

### III. RESULTS AND DISCUSSION

According to the material and methods in the above section, two different kinds of schemes were applied to acquire a detector signal to assess the implementation of the developed DPP. Pulse generator is connected to system. The system is triggered at the falling edge of a 1 MHz pulse signal. The blue and red line represent pulse features in the time and frequency domain respectively in figure 3. The experimental result of the obtained data by using the DAQ125 is depicted in figure 3(a). The blue line is the measured pulse time and a timestamp with 8 ns is assigned with 512 samples in the above curve. The red line indicates the accordant power spectrum after applying the Fast Fourier Transform (FFT) algorithm to the processing data. As a comparative outcome, the figure 3(b) represents the time and frequency information of the identical signal under a equivalent status by using HDO4000A.

As a comparison for the different schemes, the blue curve in figure 3(a) is much noisier than the one in figure 3(b) within

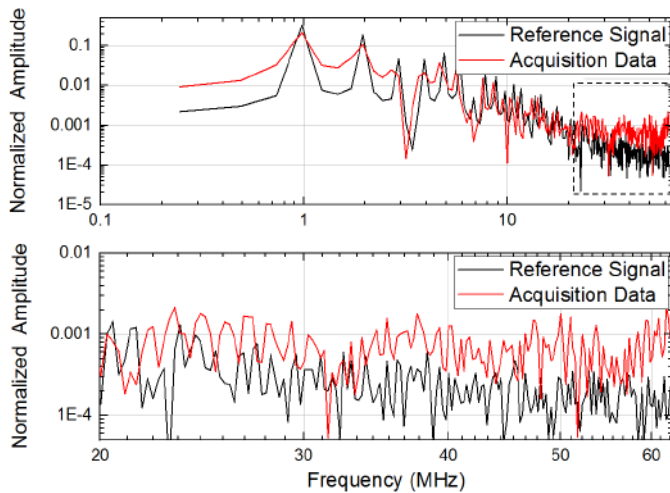


Fig. 4. Amplitude spectrogram comparison of acquired data and reference signal.

4.096  $\mu\text{s}$  sampling time. Consequently, the trend of both power spectrum curves indicate well matching in the lower frequency part, while a higher level is demonstrated in figure 3(a) than figure 3(b) at the high frequency part. For analyzing the system operation of DPP, the normalized amplitude spectrogram is presented in figure 4, which is a direct comparison of the acquired data and the reference signal in the frequency domain. The red plot exhibits data from DAQ125 and the black one displays the signal from the reference system. As can be seen from the amplitude spectrogram, FFT of the 1 MHz periodic signal is composed of a series of discrete spectral lines, all of which are integer multiples of 1 MHz. The amplitude spectrogram envelope of the acquisition data is determined by the pulse duty cycle, whose normalized amplitude is bigger than the one of the reference signal in the frequency section between 20 MHz and 62.5 MHz. Zoom of this piece is shown in the bottom graph of figure 4. It displays a regular harmonic envelope on the frequency-amplitude axis and has an offset noise above the reference signal. This graph indicates that noise suppression is necessary in the high frequency portion which is a harmonic envelope of the pulse. To analyze the system noise level and its distribution, the difference of system noise between DAQ125 and the reference system is measured in the following section.

The acquisition without input signal are extracted by using both DAQ125 and the reference system to measure and process the system noise. The display of signals based on different systems in the time and frequency domain are shown in figure 5. After calculation, the standard deviation and mean of acquisition data is 4.826 mV and 9.093 mV while the values of reference are 1.428 mV and 54.029 mV. From measurements, the system noise amplitude of DAQ125 has a wider range of floats above and below the mean of 9.093 mV which means system noise level of DAQ125 is higher than the reference system. This inference is verified by the normalized amplitude spectrogram of noise in figure 5(b). It indicates that the system noise of the DAQ125 has a higher value than the signal of the reference system in the whole frequency domain.

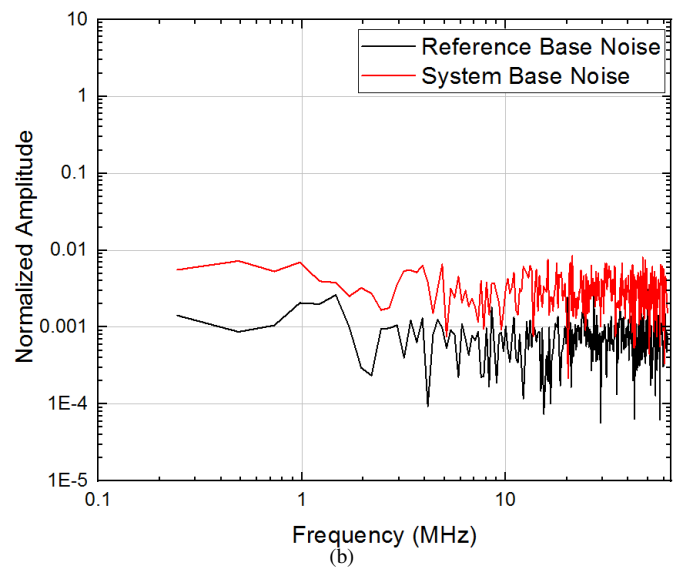
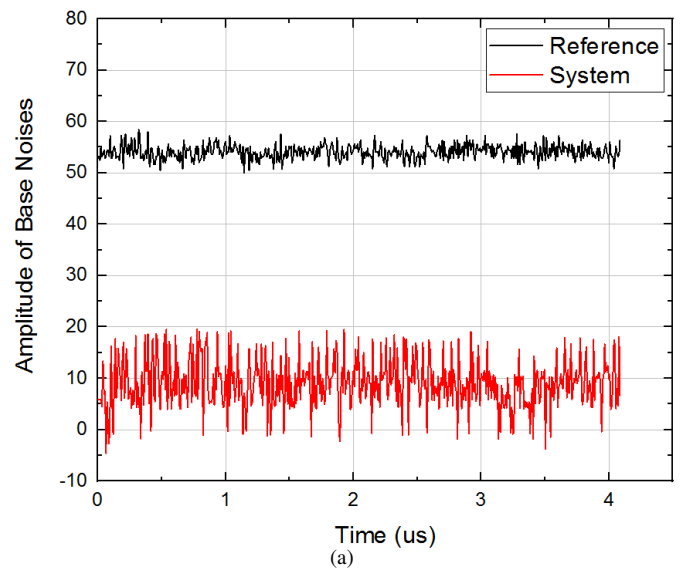


Fig. 5. Acquired data (a) and reference signal (b) shown in time and frequency domain. The total measurement is 512 samples.

A low pass filter is adopted in analog stage while a moving average filter is introduced in digital circuit block to suppress the distribution of system noise. After processing and calculation, the comparison of raw pulses and pulses from the digital filter is depicted in figure 6(a). Their  $\gamma$  spectrum with the scintillation detector  $\text{CeBr}_3$  is shown in figure 6(b). As predicted, the moving average filter has reduced the amplitude of baseline noise. The resolution at 662 keV  $\gamma$ -rays is 4.7% with radiation source  $^{137}\text{Cs}$ .

Simultaneously, radiation pulse and energy spectrum are provided in figure 7 with semiconductor detector HPGe and  $^{152}\text{Eu}$  radiation source. A trapezoidal filter is exploited for the use with a charge sensitive preamplifier in HPGe detector. The transformation after different filters is shown in figure 7(a). The figure 7(b) shows low energy part of X-rays acquired by DAQ125 system and MCA DT5780. The orange curve in figure 7(b) is the reference from the MCA DT5780 while the blue one is the acquired data from DAQ125. The first two

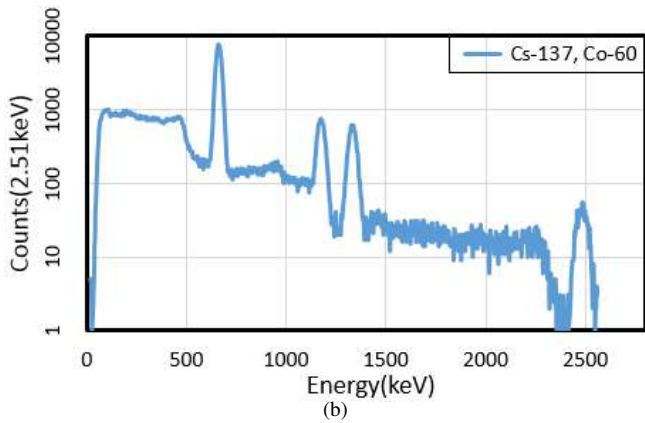
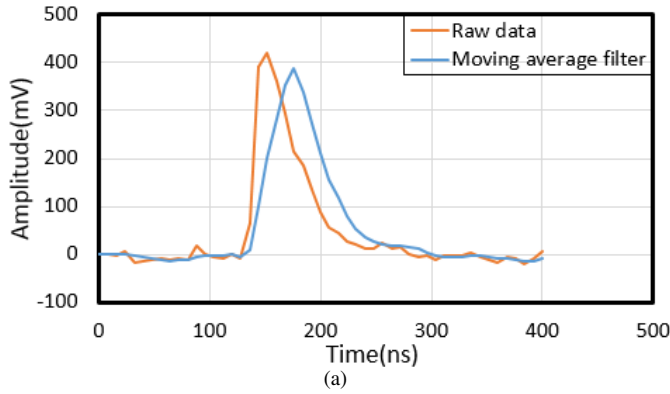


Fig. 6. Radiation pulse(a) and  $\gamma$ -rays spectrum(b) with a  $\text{CeBr}_3$  detector.

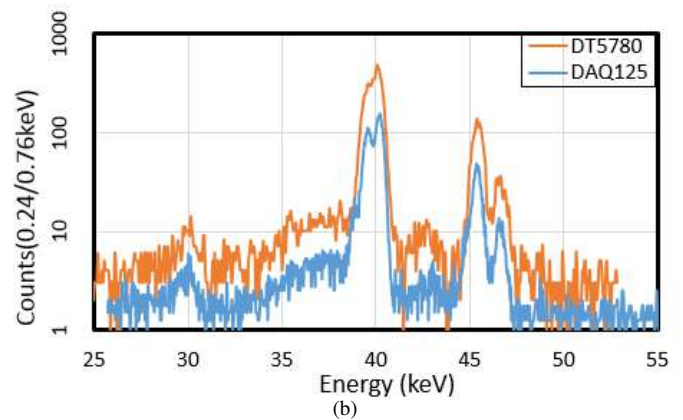
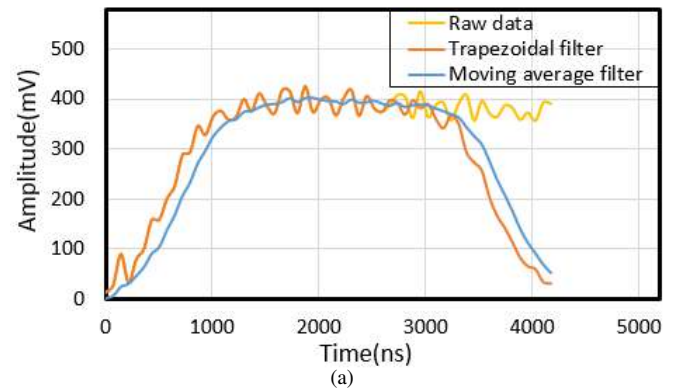


Fig. 7. Radiation pulse(a) and X-rays spectrum(b) with a HPGe detector.

peaks, 39.5 keV and 40.1 keV, are discriminated on the blue line but overlapped in orange line. Meanwhile, the acquired data from DAQ125 shows better performance at peaks 45.4 keV and 46.6 keV since they are separated much deeper than the data from MCA DT5780. As a comparative outcome, the blue plot shows a good energy resolution on the spectrum. The full width at half maximum (FWHM) is calculated at different energy using multiple radioactive source, such as  $^{152}\text{Eu}$ ,  $^{137}\text{Cs}$ ,  $^{207}\text{Bi}$ ,  $^{133}\text{Ba}$  and  $^{241}\text{Am}$ . Based on measured results and corresponding FWHM, energy resolution of HPGe detectors versus  $\gamma$ -ray energy is plotted in figure 8. It indicates that the range of energy resolution is from 0.23% to 1.00% in the energy of incident  $\gamma$ -ray with HPGe detector.

#### IV. CONCLUSION

The experiment and analysis results of DPP module for nuclear instrument are illustrated in this work. The measurement results of system noise is analyzed. Based on this analysis, a corresponding low pass filter and moving average filter are exploited in analog and digital circuit block respectively. Energy spectrum and resolution are presented with scintillating and semiconductor detector applied in nuclear instrumentation.

#### REFERENCES

[1] J. B. Simões and C. M. B. A. Correia, "Pulse processing architectures," *Nucl. Instrum. Meth.*, vol. A 422, pp. 405–410, 1999.  
 [2] W. K. Warburton, M. Momayezi, B. Hubbard-Nelson, and W. Skulski, "Digital pulse processing: New possibilities in nuclear spectroscopy," *Appl. Radiations Isotopes*, vol. 53, pp. 916–920, 2000.

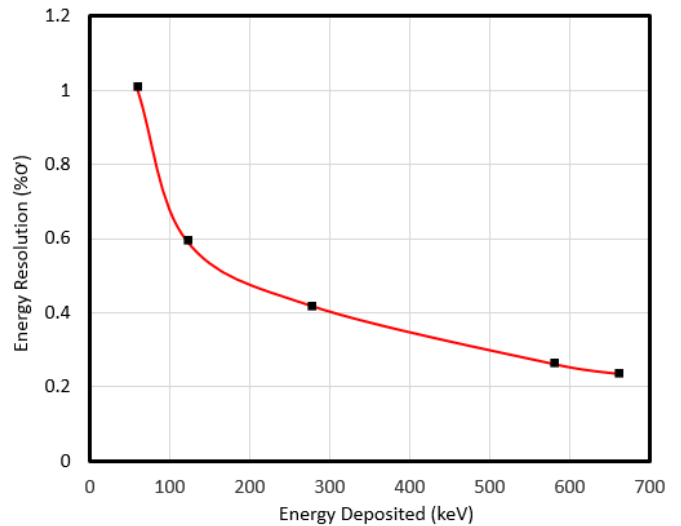


Fig. 8. Resolution range with the HPGe detector in the energy of incident  $\gamma$ -ray.

[3] J. M. Cardoso, J. B. Simões, and C. M. B. A. Correia, "A high performance reconfigurable hardware platform for digital pulse processing," *IEEE Trans. Nucl. Sci.*, vol. 51, no. 3, pp. 921–925, Jun. 2004.  
 [4] Y. Moline, M. Thevenin, G. Corre and M. Paindavoine, "A novel digital pulse processing architecture for nuclear instrumentation," *2015 4th International Conference on Advancements in Nuclear Instrumentation Measurement Methods and their Applications (ANIMMA)*, pp. 1–4, Lisbon, 2015.  
 [5] Linear Technology, "16-Bit, 125/105/80MSPS Low Power Dual ADCs," LTC2185 datasheet.